Interaction of the Gonococcal Porin P.IB with G- and F-Actin

DATASET *in* BIOCHEMISTRY · MAY 2000

Impact Factor: 3.02

Interaction of the Gonococcal Porin P.IB with G- and F-Actin†

Kuo-Kuang Wen,‡ Peter C. Giardina,§ Milan S. Blake,|| Jennifer Edwards,§ Michael A. Apicella,§ and Peter A. Rubenstein*,‡

Department of Biochemistry and Department of Microbiology, University of Iowa College of Medicine, Iowa City, Iowa 52242, and North American Vaccine, Beltsville, Massachusetts 20702-4223

Received February 2, 2000; Revised Manuscript Received May 12, 2000

ABSTRACT: The invasion of epithelial cells by *N. gonorrheae* is accompanied by formation of a halo of actin filaments around the enveloped bacterium. The transfer of the bacterial major outer membrane protein, porin, to the host cell membrane during invasion makes it a candidate for a facilitator for the formation of this halo. Western analysis shows here that gonococcal porin P.IB associates with the actin cytoskeleton in infected cells. Using the pyrene-labeled Mg forms of yeast and muscle actins, we demonstrate that under low ionic strength conditions, P.IB causes formation of filamentous actin assemblies, although they, unlike F-actin, cannot be internally cross-linked with *N*,*N*′-4-phenylenedimaleimide (PDM). In F-buffer, low porin concentrations appear to accelerate actin polymerization. Higher P.IB concentrations lead to the formation of highly decorated fragmented F-actin-like filaments in which the actin can be cross-linked by PDM. Co-assembly of P.IB with a pyrene-labeled mutant actin, $S_{265}C$, prevents formation of a pyrene excimer present with labeled $S_{265}C$ F-actin alone. Addition of low concentrations of porin to preformed F-actin results in sparsely decorated F-actin. Higher P.IB concentrations extensively decorate the filaments, thereby altering their morphology to a state like that observed when the components are copolymerized. With preformed labeled $S_{265}C$ F-actin, P.IB quenches the pyrene excimer. This decrease is prevented by the F-actin stabilizers phalloidin and to a lesser extent beryllium fluoride. P.IB's association with the actin cytoskeleton and its ability to interact with and remodel actin filaments support a direct role for porin in altering the host cell cytoskeleton during invasion.

Neisseria gonorrheae is a sexually transmitted mucosal pathogen of humans. This Gram (−) organism colonizes and invades the reproductive mucosal epithelium of men and women, causing gonorrhea and occasionally disseminating to distal tissues. Several surface-expressed gonococcal factors have been shown to affect attachment and invasion of these epithelial surfaces including opacity-associated (Opa) protein, pili, lipooligosaccharide (LOS), and protein III (PIII) (*1*). Gonococcal invasion of these epithelial surfaces likely involves a receptor-mediated endocytic process (*2*−*7*), although small numbers of gonococci have been shown to invade urethral epithelial cells via macropinocytosis (*8*). Invasion of several cell lines is accompanied by formation of transient focal rearrangements of the host actin cytoskeleton (termed actin footprints) in proximity to invading bacteria (*9*−*12*).

Recently it was shown that gonococcal porins influence bacterial invasion in a nucleotide-dependent fashion (*13*), an observation that directly correlates with the ability of gonococci to cause disseminated disease (*14*). These porins, through their involvement in phagosome maturation, have also been shown to affect the endocytic pathway in cultured human cells (*15*, *16*). These results are intriguing in light of evidence that *Neisseria*-encoded porins translocate from the bacterial outer envelope into host cell membranes during infection (*17*−*20*). In fact, porins have been shown to affect several aspects of normal host cell functions including ion flux, receptor expression, and actin dynamics (*21*−*27*).

Gonococci express a single homo-trimeric porin, PorB (35−37 kDa), as either allele P.IA or allele P.IB (*28*−*30*). Porins are abundant outer membrane proteins that control the flux of small solutes such as nutrients and ions across biological membranes in a nucleotide-dependent fashion. The primary structures of these porins are nearly identical with the exception that P.IB contains an extra 17 amino acid segment enriched in hydrophilic residues. This region is thought to reside in an extracellular loop.

Porin's abundance, its spontaneous translocation into host cell membranes during infection, and the effects it causes on ion fluxes and cytoskeletal organization suggested that during infection it interacts with and causes changes in the actin cytoskeleton. To begin to address this hypothesis, we have assessed, in this study, the interaction of gonococcal porin P.IB (isolated from strain MS11) with pyrene-labeled G-actin and F-actin.

† Supported in part by NIH grants to P.A.R. (GM33689), to M.A.A. (AI43924), and to M.A.A. and P.A.R. (AI45728), by a Muscular Dystrophy Association grant to P.A.R., by an American Heart Association Iowa Affiliate Predoctoral Fellowship to K.-K.W., and by an NIH Postodoctoral Training Fellowship to P.C.G. (AI-07343).

* Correspondence should be addressed to this author at the Department of Biochemistry, University of Iowa College of Medicine, 51 Newton Rd., Iowa City, IA 52242. Tel. (319)-335-7911; Fax (319)-335-9570; E-mail peter-rubenstein@uiowa.edu.

‡ Department of Biochemistry, University of Iowa College of Medicine.

§ Department of Microbiology, University of Iowa College of Medicine.

|| North American Vaccine.

10.1021/bi000241j CCC: $19.00
Published on Web 06/27/2000

MATERIALS AND METHODS

Materials. The Ca forms of yeast WT, $S_{265}C$, and $S_{265}C/C_{374}A$ actin were prepared by a combination of DNase I affinity chromatography and DEAE-cellulose chromatography according to Cook et al. (*31*). Rabbit skeletal muscle actin in the Ca-form was the generous gift of Larry Tobacman (University of Iowa). Ca-actin was converted to the Mg-form prior to use by the procedure of Strzelecka-Golaszewska et al. (*32*). The WT actin was labeled on Cys_{374} with pyrene-maleimide (Sigma Chemical Co., St. Louis), $S_{265}C$ actin was labeled on both Cys_{265} and Cys_{374}, and $S_{265}C/C_{374}A$ was labeled solely on C_{265} as described previously (*33*). The extent of labeling was between 75 and 100%. Porin P.IB from *N. gonorrheae* strain MS11 was purified as a homogeneous preparation in a buffer containing 25 mM Tris-HCl, pH 8.0, 0.05% Zwittergent 3-14 (Calbiochem), and 200 mM NaCl according to Gotschlich et al. (*34*). It was stored at concentrations not exceeding 1 mg/mL. Porin concentrations were calculated based on the molecular mass of the monomer, 35 kDa. Ca-G-buffer (low ionic strength) is 10 mM Tris-HCl, pH 7.5, containing 0.1 mM dithiothreitol, 0.2 mM $CaCl_2$, and 0.2 mM ATP. Mg-G-buffer is the same except that 0.2 mM $MgCl_2$ has been substituted for the $CaCl_2$. F-buffer (high ionic strength) is G-buffer to which has been added $MgCl_2$ and KCl to final concentrations of 2 and 50 mM, respectively.

Immunoprecipitation. Ectocervical tissue biopsies were obtained from premenopausal women undergoing hysterectomy at the University of Iowa Hospital and Clinics (Iowa City, IA). Tissues were used to seed primary, human ectocervical-derived cell monolayers (to be described elsewhere). Primary cells were allowed to grow to near-confluence in 35 mm tissue culture dishes after which they were infected at a multiplicity of infection of 100, for 2 h, with *N. gonorrheae* strain 1291, or they were left uninfected. Infected and uninfected cervical cells were washed at room temperature with phosphate-buffered saline (PBS). All subsequent steps were performed on ice with ice-cold reagents. Cervical cells were lysed with radioimmunoprecipitation assay (RIPA) buffer [1× PBS, 0.5% Nonidet P-40 (NP-40), 0.1% SDS, 1 mM phenylmethylsulfonyl fluoride (PMSF)]. Lysis was facilitated by passage of the cell extract through a 21 gauge needle. The cell lysate was incubated at 4 °C overnight,with rotation, in the presence of an anti-actin, goat, polyclonal IgG antibody (Santa Cruz Biotechnology Inc., Santa Cruz, CA). GammaBind Plus Sepharose (Amersham Pharmacia Biotech AB, Uppsala, Sweden) was added to the cell lysate, and incubation was allowed to continue at 4 °C, with rotation, overnight. Control *N. gonorrheae* infected cell lysates were incubated as described above with the exception that the anti-actin antibody was omitted. Immunocomplexes were recovered by a 5 min centrifugation at 2500 rpm. The supernatant was discarded, and the pellet was washed 3 times with RIPA buffer (more stringent wash) or PBS (less stringent wash). With each subsequent wash, the pellet was collected by centrifugation (2500 rpm, 5 min), and the supernatant was discarded. The final pellet was resuspended in denaturing electrophoresis buffer, boiled for 5 min, and separated on an SDS 12% to 4% gradient polyacrylamide gel. Western blotting was subsequently performed using the murine monoclonal antibodies to gonococcal porin, 3H1, monoclonal antibody 6B4 which recognizes a conserved Galβ1−4GlcNAc residue on gonococcal LOS, and monoclonal antibody 4B12 which recognizes a conserved epitope on gonococcal opacity protein. A control which omitted the primary antibody was included in each experiment. Immunocomplexes were detected with Super-Signal West Pico Chemiluminescent Substrate (Pierce, Rockford, IL) and autoradiography.

Fluorescence Spectroscopy. Fluorescence measurements of pyrene maleimide labeled proteins were obtained at 25 °C on a Spex Fluorolog 3 instrument with a thermostated cell holder (*35, 36*). For polymerization experiments, the excitation wavelength was 365 nm and the emission wavelength 386 nm. In experiments using $S_{265}C$ or $S_{265}C/C_{374}A$ actin, the fluorescence spectra were recorded from 375 to 550 nm. The total sample volume was 120 μL, and for all samples, the final Zwittergent concentration was 0.002%. For polymerization experiments, the appropriate amount of porin in 5 μL of porin storage buffer was added to 2.4 μM actin in G-buffer, and the fluorescence of the sample was determined. $MgCl_2$ and KCl were then added to achieve final concentrations of 2 and 50 mM, respectively, and the increase in fluorescence was observed as a function of time. The steep deflection observed at the beginning of kinetic traces following the addition of salt to induce polymerization is due to the opening and closing of the sample compartment.

Phenylenedimaleimide Cross-Linking. Covalent cross-linking of actin with *N*,*N*′-4-phenylenedimaleimide (PDM) in the presence and absence of porin was carried out using a modification of the procedures described previously (*37*−*39*). Actin was dialyzed against DTT-free G-buffer prior to use in these experiments to remove exogenous reactive thiol groups. Three microliters of a 500 μM solution of PDM in dimethylformamide was added to 60 μL of a 2.5 μM actin solution free of DTT in the presence or absence of 1.2 μM porin either before or at the completion of the salt-induced polymerization reaction. The final concentration of cross-linker was 24 μM, giving a cross-linker:actin ratio of about 10:1. After 8 min at 25 °C, the reaction was quenched with 20 μL of a solution containing 20% β-mercaptoethanol, 0.25 M Tris-HCl, pH 6.8, 4.6% SDS, 0.02% bromophenol blue, and 40% glycerol. Samples were then resolved electrophoretically on 10% polyacrylamide gels in SDS, and the proteins were visualized by Coomassie Blue.

Electron Microscopy. Samples containing 2.4 μM actin were deposited on carbon-coated Formvar grids, negatively stained with 1.5% uranyl acetate, and observed on a Hitachi 7000 transmission electron microscope in the University of Iowa Central Electron Microscopy Facility.

RESULTS

Immunoprecipitation of P.IB Associated with the Actin Cytoskeleton in Vivo. Previous studies in our laboratory demonstrated the transient appearance of "actin footprints" surrounding gonococci as they entered human urethral epithelial cells (*7*). To determine if the actin cytoskeleton interacted with gonococcal surface components directly, we performed immunprecipitation experiments in which actin from infected cells that was captured with a rabbit anti-actin antibody was probed by Western blotting with monoclonal antibodies to gonococcal porin, lipooligosaccharide (LOS),

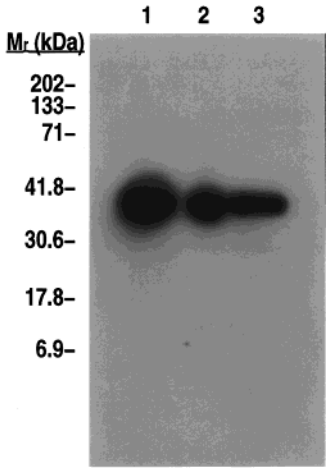

FIGURE 1: P.IB from *N. gonorrheae* associates with the actin cytoskeleton in infected human ectocervical cells. Actin was immunoprecipitated from detergent-lysed cells with an anti-actin antibody, and following separation of the components of the immunoprecipitate by SDS−PAGE, the P.IB was visualized using an anti-porin antibody as described under Materials and Methods. Lane 1, P.IB alone; lane 2, pellet was washed under stringent (RIPA) conditions prior to electrophoresis; Lane 3, pellet was washed under less stringent (PBS) conditions.

and opacity protein. Figure 1 shows the Western blot analysis of the washed actin−anti-actin immunocomplexes with the anti-gonococcal porin antibody 3H1. In controls in which primary antibody was omitted, no such association was detected. These studies show the ability of porin to associate with the actin cytoskeleton in infected cells. Similar studies performed using monoclonal antibodies 3F11 or 4B12 which recognize conserved epitopes on gonococcal LOS and opacity protein, respectively, were negative.

Having established that P.IB can associate with the actin cytoskeleton in vivo, we wished to determine whether porin could directly interact with actin. The following studies are based largely on the change in fluorescence caused by the interaction of *N. gonorrheae* P.IB with yeast actin labeled at C_{374} with pyrene maleimide. In these experiments, any changes we observe in fluorescence reflects changes in the environment of the fluorescent probe on the actin and does not report on the structure of the porin. We maintained constant Zwittergent concentrations in all assays. The use of yeast actin for the bulk of our studies is justified because it is 88% homologous with mammalian skeletal muscle actin (*40*), will translocate over muscle myosin in an in vitro motility assay (*41*), and forms an interaction with myosin that can be regulated by Ca in the presence of tropomyosin and troponin (*42*).

Interactions in G-buffer. We first mixed increasing amounts of P.IB with pyrene maleimide labeled yeast Mg-G-actin under low ionic strength conditions (G-buffer) in which actin itself will not polymerize. Furthermore, there was no evidence of actin aggregation or assembly in the presence of the Zwittergent concentrations used in these low ionic strength studies. Figure 2 shows that at porin concentrations above about 0.5 μM (actin:porin ratio = ~5:1), there was a concentration- and time-dependent increase in actin fluorescence. Such an increase is not due to the presence of detergent in the buffer, since controls show that the fluorescence of actin is the same whether detergent is present. These results suggested that in low ionic strength conditions

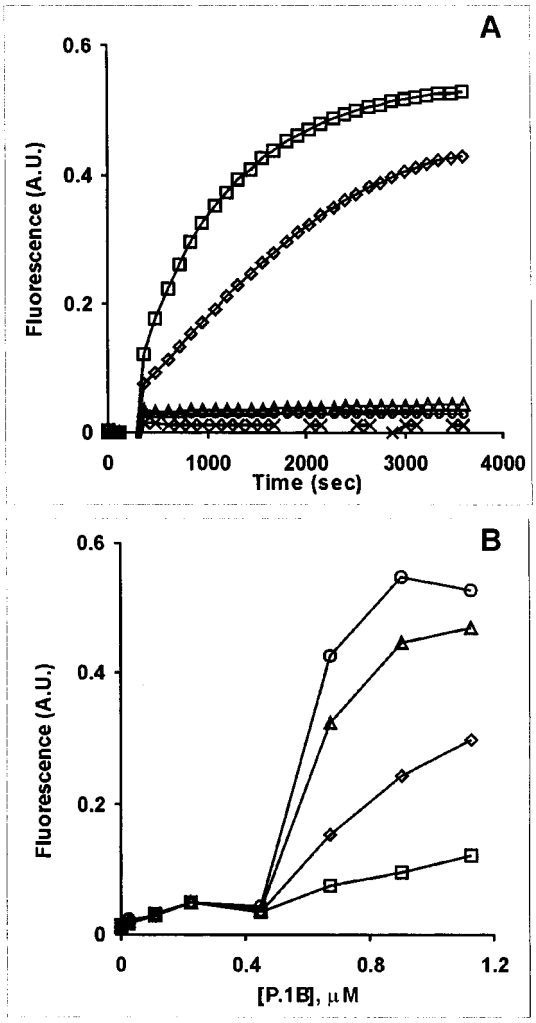

FIGURE 2: Interaction of P.IB with pyrene-labeled Mg-G-actin in low ionic strength solution. (A) The fluorescence change in 2.4 μM pyrene-labeled Mg-G-actin caused by differing concentrations of P.IB was assessed as a function of time: (□) 1.2 μM; (◊) 0.7 μM; (△) 0.45 μM; (○) 0.1 μM; (×) no porin. (B) Time dependence of the fluorescence change in 2.4 μM pyrene-labeled Mg-G-actin caused by increasing amounts of porin: (□) 2 min; (◊) 10 min; (△) 30 min; (○) 60 min.

with Mg-G-actin, P.IB may mediate some type of self-association process involving actin, even though ionic conditions were such that, in the absence of P.IB, actin polymerization did not occur.

Electron micrographs showed that this increased fluorescence was accompanied by the appearance of filament-like arrays of material (Figure 3) with morphology different than that of F-actin. There seemed, instead, to be linear depositions of short fragments. No such material was observed with actin alone or with porin alone under the same conditions or in the absence of detergent. The failure of these filaments to form with actin alone either in the absence or in the presence of detergent indicates that their presence does not merely reflect the sequestering of detergent by the porin thereby allowing the actin to self-associate.

Since the gonococci infect mammalian cells, we repeated the experiment with rabbit muscle actin to determine if the interaction we saw was specific for yeast actin. The interaction of P.IB with the Mg form of muscle actin in low ionic strength solution is similar to that observed with yeast actin

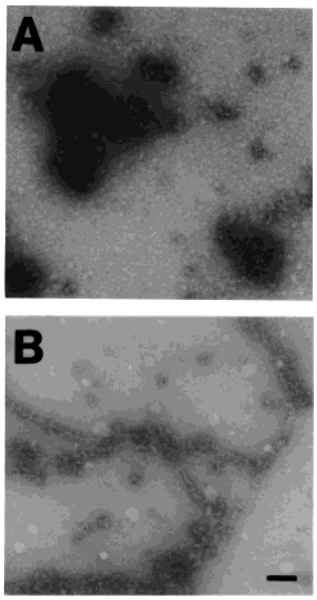

FIGURE 3: Structures formed after combining P.IB with Mg-G-actin under low ionic strength conditions. Actin (2.4 μM) was mixed with 0.5 molar equiv of the appropriate porin, and after 1 h, the sample was processed for electron microscopy as described in the text. (A) P.IB alone; (B) P.IB + actin. Bar: 0.1 μm.

in terms of fluorescence profile (Figure 4A) and EM images (not shown).

Interactions in F-buffer. We repeated the experiments previously described under more physiological conditions that promote actin assembly (F-buffer). In these experiments, we have depicted the time courses showing the salt-induced fluorescence increases as a function of porin concentration, and we have also graphed the peak fluorescence in each experiment as a function of porin concentration. Salt was added to yeast Mg-G-actin solutions containing different concentrations of P.IB to induce polymerization, and the rate and extent of fluorescence increase were assessed. Figure 5 shows a marked biphasic behavior dependent on P.IB concentration. At lower P.IB concentrations, polymerization curves resembled that of actin alone although as the P.IB concentration increased, there appeared to be an acceleration of the rate of fluorescence increase. Furthermore, the peak fluorescence increased until a maximum was reached at an actin:porin ratio of 3.5:1. Further increases in porin concentration resulted in a decrease in the peak fluorescence as well as a change in the appearance of the polymerization curve. With increased porin, the pre-salt fluorescence value increased while the amount of post-addition fluorescence increase lessened. At an actin:porin ratio of 2:1, there was no increase in fluorescence beyond the value that existed before the salt was added. Figure 4B shows that 2.4 μM muscle actin in the presence of 1.2 μM porin exhibited a behavior similar to that of yeast actin under the same conditions.

We next examined solutions containing different amounts of porin by electron microscopy following the cessation of the assembly process. At lower porin concentrations, we observed undecorated and partly decorated long actin filaments as well as shorter and thicker decorated filaments (Figure 6B). At higher porin concentrations, we observed only numerous loosely associated short fragments and only very few undecorated filaments (Figure 6C). The same

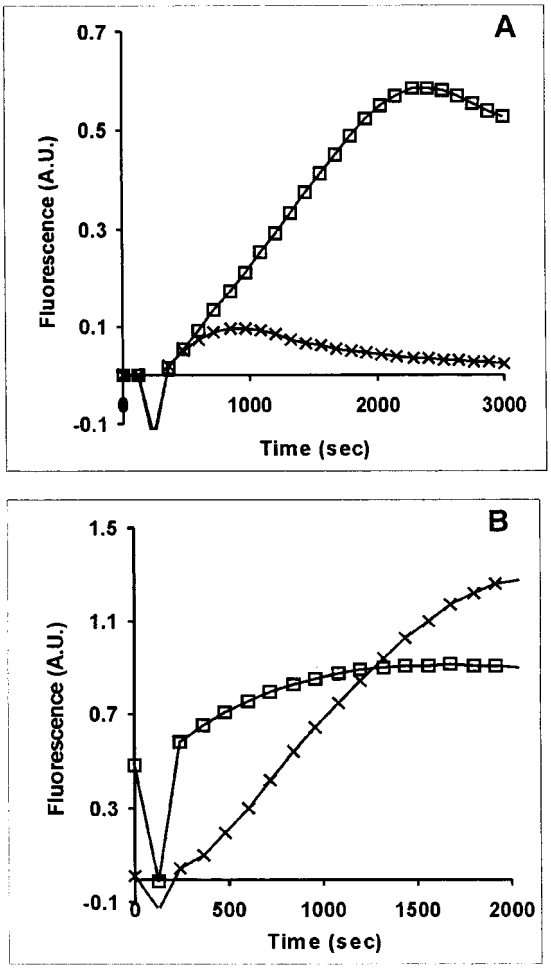

FIGURE 4: Interaction of 1.2 μM P.1B with 2.4 μM pyrene-labeled rabbit skeletal muscle actin. The two proteins were combined in G-buffer and followed by fluorescence in panel A or following addition of salts to bring the solution to F-buffer conditions in panel B. (□) P.IB; (×) no porin.

behavior was observed when P.IB was copolymerized with muscle Mg-G-actin in F-buffer (data not shown).

Interaction of Porin with Preformed F-Actin. We determined whether P.IB could interact with preformed yeast Mg-actin filaments, and, if so, whether it had an effect on filament morphology. F-Actin and porin were gently mixed in F-buffer, and aliquots were removed at different times, deposited on carbon-coated EM grids, and negatively stained with uranyl acetate. Figure 7 shows that immediately after mixing, there were well-spread arrays of tightly coated filaments. Between 15 and 20 min after the addition of porin, the filaments began to show evidence of fragmentation and/or disorganization. This process was largely complete by 30−40 min. The latter samples looked very similar to those formed by the copolymerization of P.IB and Mg-G-actin under high ionic strength conditions. This experiment was performed twice using different preparations of actin with identical results. Experiments with preformed muscle F-actin showed results qualitatively similar to those observed with the yeast F-actin (data not shown).

N,N′-4-Phenylenedimaleimide (PDM)-Dependent Cross-Linking of Actin in P.IB/Actin Mixtures. Because of the morphological differences in the filaments elicited by P.IB in low and high ionic strength solutions compared with F-actin, we examined the ability of the actin in these

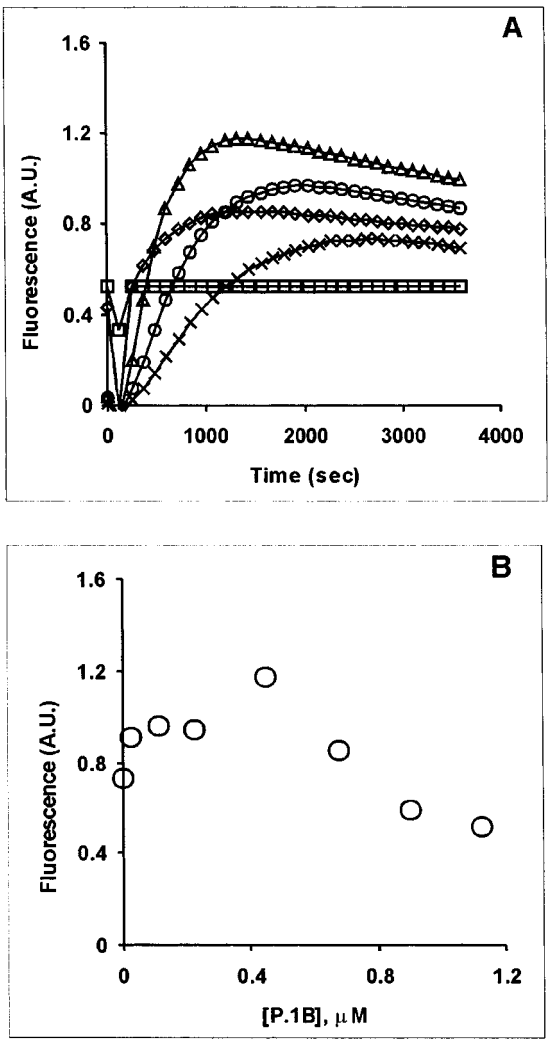

FIGURE 5: Interaction of differing concentrations of P.IB with 2.4 μM Mg-G-actin following addition of F-salts. (A) (□) 1.2 μM; (◊) 0.9 μM; (△) 0.7 μM; (○) 0.4 μM; (×) no porin. (B) Peak fluorescence values from the curves in panel A were graphed as a function of porin concentration.

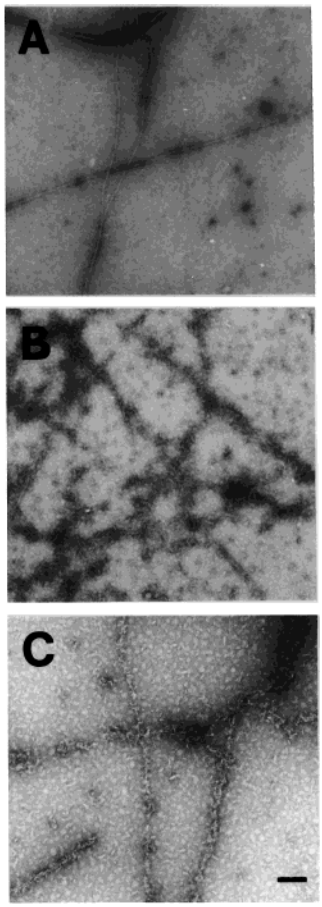

FIGURE 6: Structures formed by combining 2.4 μM Mg yeast actin with differing amounts of P.IB following addition of polymerization-inducing salts. Samples were prepared 1 h after the addition of salt. Panel A, F-actin alone; panel B, 0.6 μM P.IB; panel C, 1.2 μM P.IB. Bar: 0.1 μm

aggregates to be cross-linked by PDM (*37, 38*). In F-actin, this reagent cross-links neighboring actins in one of two ways to give an upper dimer of apparent MW about 115 K and a lower dimer of about 86 K. The lower dimer is much more evident during the early stages of polymerization. The upper dimer, which represents cross-linking between adjacent monomers in the same strand along the filament axis, is the major species late in the polymerization reaction (*39*). Under low ionic strength conditions in the presence or absence of P.IB, no cross-linking was observed (Figure 8A), even though EM shows that filamentous material was abundant. However, when P.IB was co-assembled with G-actin under high ionic strength conditions (Figure 8B) or was added to preformed F-actin (Figure 8C), an upper dimer band signifying the cross-linking of actins was clearly evident. Furthermore, the extent of cross-linking was approximately the same as that achieved with F-actin alone (Figure 8C, lane 1). These results indicate that under higher ionic strength conditions, the actin/porin assemblies involve elements of F-actin structure.

The extent of cross-linking we observed is less than but near to that reported previously with PDM (*37*−*39*). In our case, as opposed to the original studies with muscle actin, we are performing the reaction at substantially lower pH in detergent, with a different actin known to have different polymerization properties, and at a lower actin concentration in which a significant percentage of the actin present may be in the G-form. All of these factors would be expected to decrease the efficiency of cross-linking achieved. However, the results are still meaningful since G-actin alone does not show the cross-linking whereas F-actin does, and the extent of cross-linking in co-assembled samples of actin and porin in F-buffer equals that seen in the absence of the porin under the same conditions.

Interaction of P.IB with Pyrene-Labeled Yeast $S_{265}C$ and $S_{265}C/C_{374}A$ Actin under Low Ionic Strength Conditions. To further investigate the extent to which P.IB might have altered the F-actin structure, we made use of two mutant yeast actins. Previously, we constructed a mutant yeast actin $S_{265}C$ (SC) in which a cysteine residue was substituted for the conserved S_{265} (*33*). This residue is adjacent to a hydrophobic plug believed to be important in actin helix stabilization by forming a bridge to a hydrophobic surface comprised of the interface of two monomers on the opposing strand (Figure 9). C_{265} is on the side of the actin monomer opposite that of C_{374} which lies on a flexible arm between subdomains 1 and 2. Reaction of this actin with pyrene maleimide resulted in the labeling of both C_{265} (loop probe) and C_{374} (C-terminal probe). Polymerization led to the formation of a pyrene excimer band with a peak at 485 nm. This new band results from a stacking interaction between

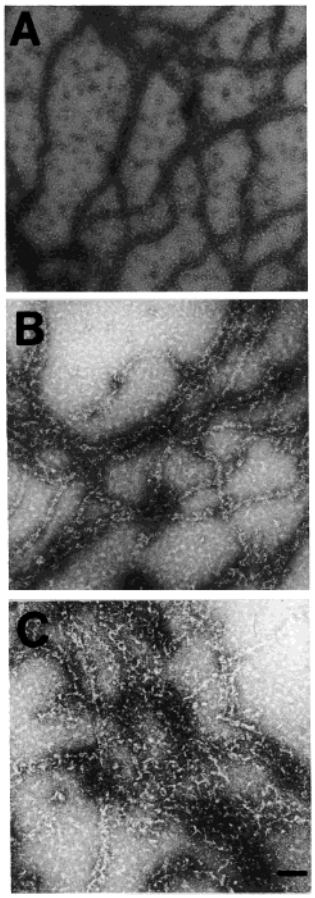

FIGURE 7: Electron micrographs depicting the interaction of 1.2 μM P.IB with preformed 2.4 μM Mg yeast F-actin. Times shown are the period elapsed following gentle mixing of the porin with preformed F-actin in F-buffer. Sample preparation is described under Materials and Methods. The actin by itself appears as that shown in Figure 6. (A) 0 min; (B) 15 min; (C) 30 min. Bar: 0.1 μm.

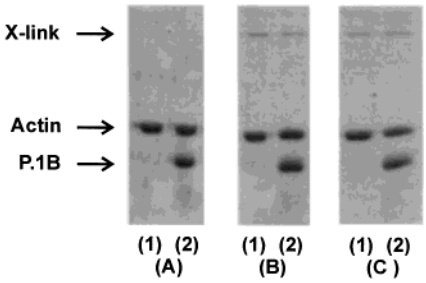

FIGURE 8: Cross-linking of actin/P.IB mixtures with PDM. Actin (2.4 μM), either in detergent buffer alone (lane 1) or in the presence of 1.2 μM P.IB (lane 2), was reacted with PDM as described under Materials and Methods, and the reaction products were resolved by SDS gel electrophoresis on 10% acrylamide gels and stained with Coomassie Blue. Panel A: G-buffer alone. Panel B: the actin and porin were combined in G-buffer for 1 h, and salt was added to induce polymerization. Panel C: Preformed F-actin in F-buffer was combined with P.IB for an additional hour.

the loop probe of one monomer with the C-terminal probe of another monomer in the opposing helical strand (*33*). The loop probe was apparently forced into the interstrand space of the actin helix where it could interact with the C-terminal probe of another actin monomer. The geometry for this interaction requires a space of 18.5 Å between the sulfur atoms of the two labeled cysteines which is possible only in the context of F-actin (*43*).

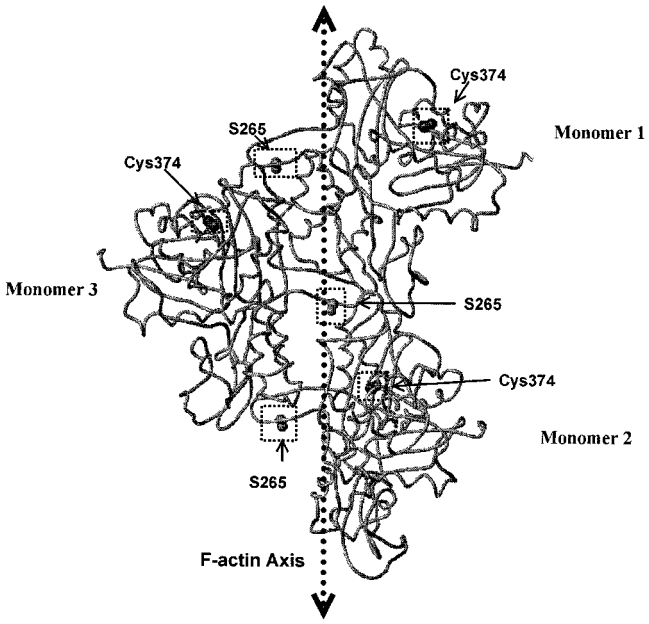

FIGURE 9: Model of F-actin (*42*) showing three actin monomers and the positions of residue 265 on the subdomain 3/4 loop as well as residue 374 adjacent to the C-terminus of the protein. These residues are the sites of attachment of the pyrene maleimide used in this study. The loop containing residue 265 is involved in a proposed hydrophobic plug−pocket interaction believed to impart stability to the filament.

A second related mutant actin, $S_{265}C/C_{374}A$ (SCCA), eliminated the reactive C-terminal Cys so we could study the loop probe alone. Polymerization of labeled SCCA actin resulted in a decreased fluorescence of the loop probe, consistent with the hypothesis that polymerization caused it to sample the more hydrophilic interstrand space within the actin helix (*33*).

The combination of P.IB with labeled SCCA actin under low ionic strength conditions resulted in a concentration-dependent increase in fluorescence of the actin loop probe (Figure 10A). This result suggests that the porin formed an association with actin that caused the loop probe to occupy a different environment than seen with F-actin alone. Repetition of the experiment with labeled SC actin (Figure 11A) resulted in a lack of appearance of the excimer in addition to an increased fluorescence of the normal pyrene bands at 386 and 395 nm, well above that which would be expected with the C-terminal probe alone. This result, coupled with our PDM cross-linking data, indicates that at the end of the reaction, the filamentous material observed in low ionic strength solutions at higher porin concentrations is not F-actin.

Co-assembly of P.IB with Pyrene-Labeled Yeast $S_{265}C$ and $S_{265}C/C_{374}A$ Actin in High Ionic Strength Solutions. We then compared the results obtained with the two actins when the porin was combined with SCCA (Figure 10B) and SC G-actins (Figure 11B) and co-assembled in higher ionic strength F-buffer. The results show that as the amount of porin increases, the magnitude of the excimer band due to F-actin decreases until it disappears at the highest porin concentration used. There is also a concomitant increase in the fluorescence of the peaks at 386 and 395 nm. However, the cross-linking data indicate that under these conditions, the actin monomers maintained many of the intermonomer contacts seen with F-actin alone (Figure 8).

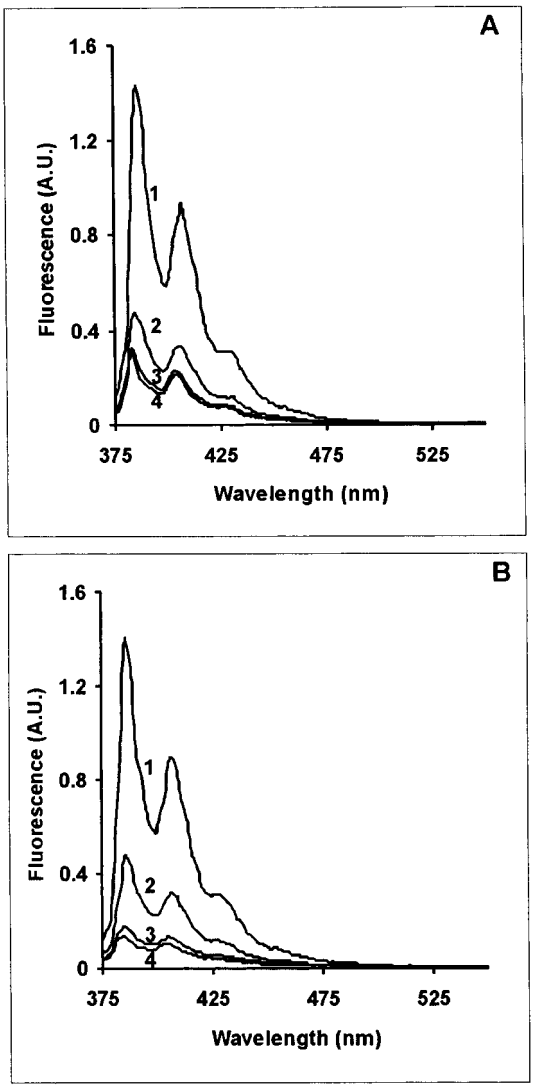

FIGURE 10: Interaction of 2.4 μM pyrene-labeled SCCA actin with differing concentrations of P.IB. Panel A: the two components were combined in G-buffer and the fluorescence spectra recorded as described under Materials and Methods. Panel B: following mixing of the two components in G-buffer for 40 min, $MgCl_2$ and KCl were added to final concentrations of 2 and 50 mM to induce actin polymerization. After an additional 40 min, the spectra were again recorded. Line 1, 1.2 μM P.IB; line 2, 0.7 μM P.IB; line 3, 0.1 μM P.IB; line 4, actin alone.

Interaction of P.IB with Pyrene-Labeled Yeast $S_{265}C$ and $S_{265}C/C_{374}A$ Preformed F-Actin. Finally, we mixed the porin with either preformed labeled SC-F-actin or SCCA-F-actin. With SCCA actin, the pyrene fluorescence of the loop probe increased as the porin concentration increased (Figure 12A). This result suggested that the porin caused a remodeling of the filament to expose the loop probe with which it could then interact. When the SC actin was used, the magnitude of the excimer peak decreased and the 386 and 395 nm bands increased as the porin concentration increased although the magnitude of the excimer peak remained substantially above zero at the highest porin concentrations (Figure 12B). We observed no increase in fluorescence when P.IB was combined with preformed pyrene-labeled WT actin labeled only at C_{374} (data not shown).

Ability of Actin Filament Stabilizing Agents To Prevent the Porin-Dependent Remodeling of F-Actin. The partial resistance of the preformed actin filament to porin-dependent remodeling suggested that filament stabilizing agents might enhance the extent of this resistance. Phalloidin, a mushroom toxin, strongly stabilizes actin filaments through formation of cross-strand contacts (*44*, *45*) and should prevent porin-dependent filament distortion or strand separation. Figure 13A shows no decrease in the excimer band following addition of porin to the phalloidin−actin solution, consistent with this hypothesis, even though EM shows that decorated filaments still form. Beryllium fluoride, BeFx, is a phosphate analogue which stabilizes actin monomer−monomer contacts within one strand of the helix by occupying the space produced by release of P_i following hydrolysis of bound ATP during actin polymerization (*46*). This replacement shifts the

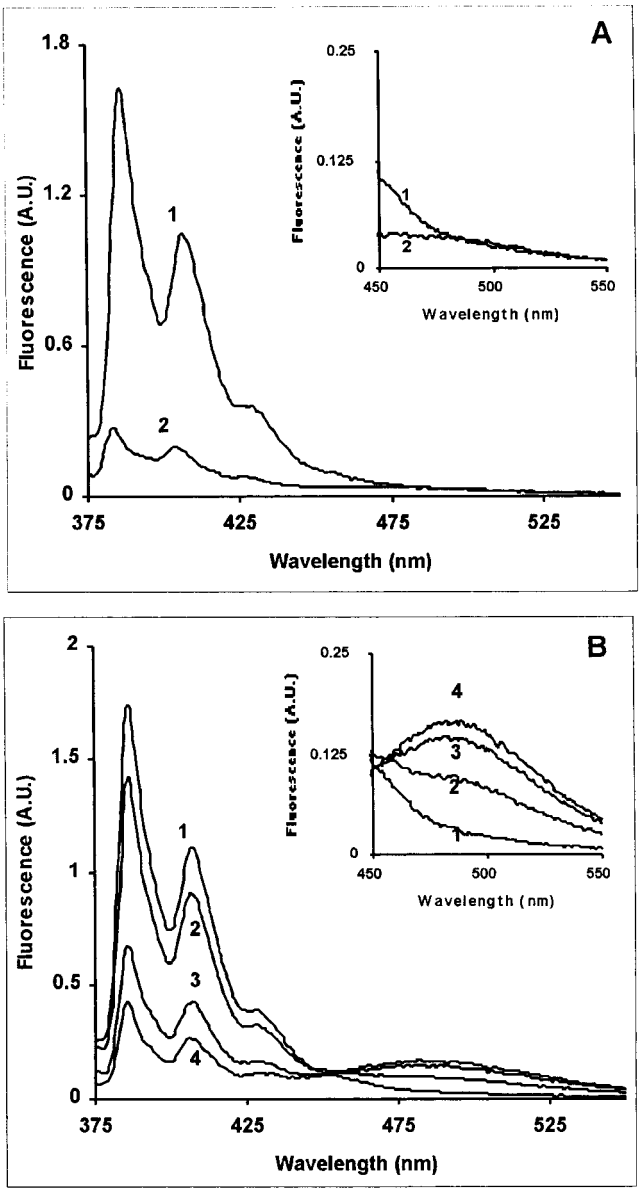

FIGURE 11: Interaction of 2.4 μM pyrene-labeled SC actin with P.IB. The insets depict amplification of the excimer region of the plots between 450 and 550 nm. Panel A: the two components were combined in G-buffer, and the fluorescence spectra were recorded as described under Materials and Methods. Line 1, 1.2 μM porin; line 2, actin alone. Panel B: following mixing of the two components in G-buffer for 40 min, $MgCl_2$ and KCl were added to final concentrations of 2 and 50 mM to induce actin polymerization. After 40 min, the spectra were again recorded. Line 1, 1.2 μM P.IB; line 2, 0.7 μM P.IB; line 3, 0.1 μM P.IB; line 4, actin alone.

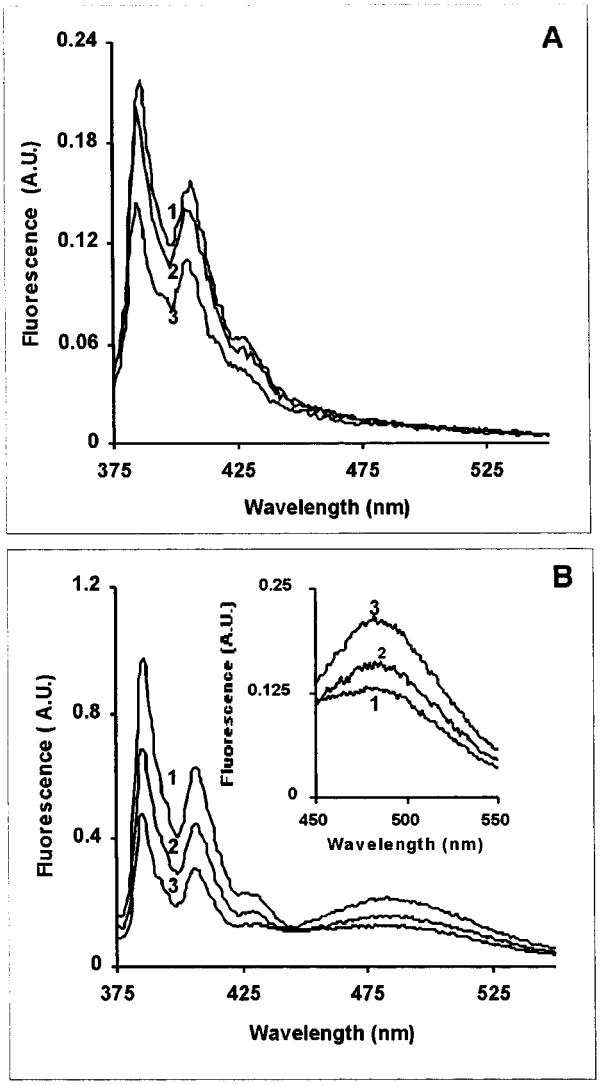

FIGURE 12: Interaction of different concentrations of P.IB with pyrene-labeled preformed SCCA (panel A) and SC (panel B) F-actin. For all experiments, the actin concentration was 2.4 μM. Fluorescence spectra were recorded 40 min after combining the actin and porin in F-buffer. The inset depicts an amplification of the excimer region of the plots between 450 and 550 nm. Line 1, 1.2 μM P.IB; line 2, 0.7 μM P.IB; line 3, actin alone.

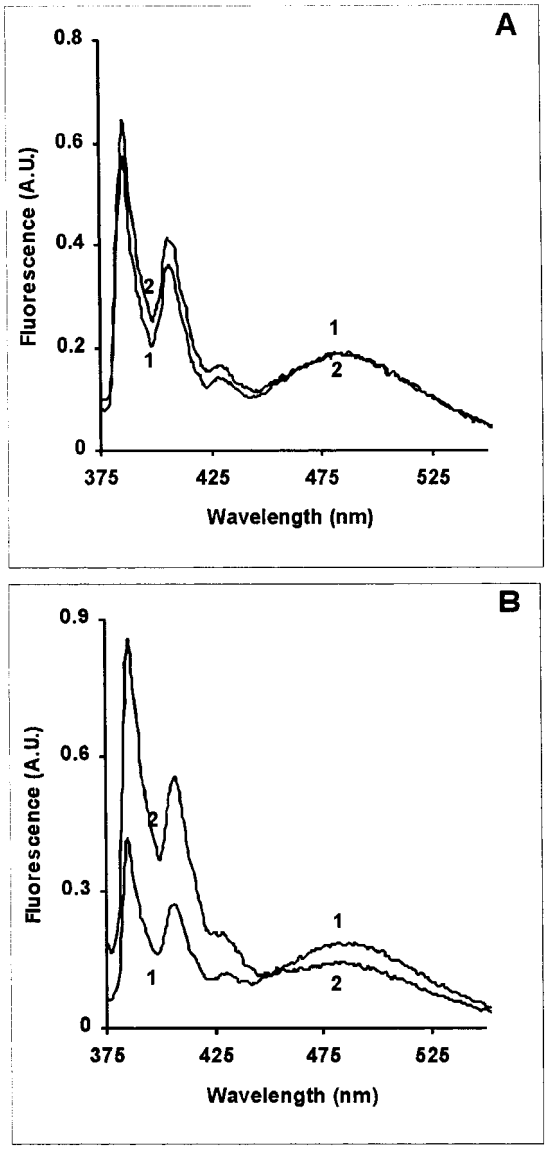

FIGURE 13: Effect of 2.4 μM phalloidin (panel A) and 0.1 mM BeFx (panel B) on the interaction of 1.2 μM P.IB with 2.4 μM pyrene-labeled preformed SC F-actin. The fluorescence spectra were recorded 40 min after mixing the two components. Line 1, actin alone; line 2, P.IB.

F-actin to a more stable ATP-like state (*47*). However, since BeFx appears to stabilize longitudinal actin monomer−monomer contacts, it should not stabilize the filament against distortion or strand separation to the same extent as phalloidin. When porin was combined with BeFx-stabilized labeled SC actin, we observed a decrease in fluorescence but one that was significantly less than occurred in the absence of the BeFx, again consistent with our hypothesis of porin-dependent remodeling of F-actin (Figure 13B).

DISCUSSION

The translocation of porin to the host cell membrane during *Neisseria* infection (*17*−*20*) and our demonstration here that porin interacts with the actin cytoskeleton in infected cells suggest a role for this protein in the rearrangement of the actin cytoskeleton that occurs during the early stages of the infective process. The results of our studies of the interaction of gonococcal porins with yeast and muscle actins are consistent with such a role.

We have shown, for the first time, using pyrene-labeled yeast actin, that P.IB can interact with either G- or F-actin and can affect the manner in which actin assembles. Based on our cross-linking studies with PDM, high concentrations of P.IB induce the formation of non-F-actin filamentous structures in G-buffer. Bringing this solution to F-buffer conditions then allows these structures to transform into filaments with elements of F-actin.

The porin-dependent changes in fluorescence of the actin C-terminal probe that occur in low and higher ionic strength solutions are complex. Polymerization of actin alone results in an increase in fluorescence. A different probe environment, resulting in a lower fluorescence yield, is produced by the interaction of porin with the actin under low salt conditions, and it appears that once this environment is established, it remains unchanged following the subsequent incorporation of the actin into a filament with F-actin-like properties. On the contrary, experiments with preformed F-actin suggest that once F-actin has formed, the porin-dependent probe environ-

ment cannot be reached, even though other studies indicate that a remodeling of the filament occurs. The copolymerization experiments involving a given amount of actin with different concentrations of porin can thus be interpreted based on these results. Prior to salt addition, for a given amount of actin, the initial fluorescence signifying the porin-dependent environment will increase as the porin concentration increases, leaving less unassociated actin available to produce the usual polymerization curve seen with pyrene actin alone. At concentrations of porin where all of the actin is associated with P.IB prior to the addition of salt, the porin-associated actin can be driven into an F-actin-like state without a concomitant change in fluorescence. This interpretation is also consistent with the results we obtained by following changes in the excimer band using pyrene-labeled SC actin.

Experiments with pyrene-labeled SC and SCCA mutant yeast actins revealed that the topologies of these actin filaments, produced in high ionic strength conditions, are altered in comparison with F-actin. The probe geometry in F-actin required for excimer formation coupled with the behavior of the loop probe alone suggests a structure in which the position of the labeled subdomain 3/4 loop has changed, thereby exposing the probe for possible direct interaction with porin. Alternatively, the enhanced fluorescence of the loop probe in this filamentous state may indicate that the probe has become embedded in a more hydrophobic pocket in the filament. Higher concentrations of porin seem to remodel the filaments in a manner resulting in their fragmentation or severing.

Finally, we have demonstrated by EM that at high relative concentrations (actin:porin = 2:1), P.IB can bind rapidly to preformed F-actin to form a tightly decorated filament whose topology is then altered over time while at lower concentrations, sparse decoration occurs with little apparent remodeling of the filament. PDM studies revealed that the high-porin filaments have some F-actin character like those formed when the G-actin and P.IB are induced to co-assemble following salt addition. Experiments with preformed SC F-actin revealed that filament reorganization involves a diminution although not elimination of the pyrene excimer with a concomitant increase in the fluorescence bands at 386 and 395 nm. With pyrene-labeled SCCA actin, we observed a large (4−5×) fluorescence increase when the P.IB was mixed with the actin under G-buffer conditions or co-assembled with G-actin in the presence of F-buffer. A smaller increase (∼50%) was observed when the P.IB was mixed with preformed labeled SCCA F-actin. The failure of the binding of P.IB to labeled WT F-actin actin (C_{374}) to cause such a change in fluorescence suggests that the porin-dependent F-actin remodeling is focused on the loop region near the filament center.

This is not the first time that binding of a protein to the filament has caused an increase in fluorescence of the loop probe. In our previous work (*33*), we observed that the addition of saturating amounts of myosin S1 to these filaments also produced an increase in pyrene fluorescence over what was found in the filament alone. However, in that case, the increase was < 20% of the original value, far lower than what we observed in the case of P.IB. Furthermore, the ability of this actin-binding protein to elicit this behavior is not a characteristic of actin-binding proteins in general since it is not seen with the binding of tropomyosin to these labeled actins.

Based on this fluorescence behavior, remodeling by P.IB, which is dampened by the strength of the intermonomer contacts within the F-actin helix, may involve the distortion of the filament leading to separation of the stacked pyrenes. This movement, if it occurs, must also be accompanied by a repositioning of the loop probe to somewhere other than the relatively hydrophilic environment between the two actin strands of the helix. An alternative explanation for the dampening of the excimer band is that the extent of pyrene stacking remains intact but that there is a large environmental change in the region of the stacked pyrenes resulting in a quenching of the excimer fluorescence. However, we believe this second explanation is less likely since the decrease in excimer fluorescence is accompanied by an increase in the fluorescence at 386 and 395 nm which would be expected if the probes no longer interacted directly with each other. Either model is further supported by the differential effects exerted by phalloidin and BeFx in preventing this remodeling based on the mechanisms by which they are known to interact with F-actin.

Importantly, the interaction of gonococcal porin with actin cannot be attributed merely to the nonspecific deposition of a hydrophobic protein on actin in an aqueous environment. The nature of the interaction is highly dependent on the identity of the porin itself. In work to be submitted elsewhere, we have found that Por, the porin from *H. influenzae*, although it can bind to G-actin, will not drive it into filaments. Furthermore, when Por was mixed with F-actin at concentrations that P.IB would totally coat the actin, little decoration was seen and there was no apparent remodeling of the actin when visualized by electron microscopy. Por interacted with G-actin but in a very different way, and it did not seem to drive the actin into filamentous structures, suggesting that the Por/actin interaction could be overcome by the normal actin monomer−monomer contacts within the actin helix. This Por−actin interaction that we have described, unlike the behavior of P.IB, may reflect an association that occurs normally within the eukaryotic cell. VDAC, the mitochondrial equivalent of bacterial porin, forms a voltage-dependent channel in the outer mitochondrial membrane. Colombini and co-workers (*48*) have recently reported that VDAC, in its closed form, will interact with G-actin, but not F-actin, thereby preventing opening of the channel. From these results, they suggested that within the eukaryotic cell, actin may play a role in controlling ion trafficking through the mitochondrial membrane.

The ability of an integral membrane protein to directly interact with actin is uncommon. One such example is ponticulin, a membrane-bound protein, found in *Dictyostelium discoideum*, that appears to anchor actin filaments to the cell membrane (*49*−*52*). We are unaware of a previous report of a membrane-bound bacterial protein able to interact specifically with actin. There is, however, a recent report that a *Salmonella typhimurium* cytosolic protein, SipA, is introduced into the host cell cytosol during infection and facilitates the infective process by binding directly to actin and, together with plastin, modulating cytoskeletal dynamics (*53*, *54*).

We have demonstrated in vitro that gonococcal porin can associate with G-actin, affect the kinetics of actin filament

formation, and cause remodeling of preformed actin filaments. This is significant because it demonstrates the direct interaction of a bacterial protein with actin and may serve as a model system for the interaction of eukaryotic porin-like molecules with the actin cytoskeleton. More significantly, we have observed that this interaction between P.IB and actin occurs in cultured cervical epithelial cells infected with *N. gonorrheae*. It has been suggested that the porins are important for *Neisseria* infectivity. Porins translocate into the host cell membrane during the infection process, thereby placing them in a position to interact directly either with the cortical cytoskeleton or with G-actin in the cell. These facts, coupled with our results, are consistent with the hypothesis that the porins may play a direct role in cytoskeletal remodeling during infection. However, a genetic approach will ultimately be required to directly test the molecular basis for the role of porins during infection.

ACKNOWLEDGMENT

Kuo-Kuang Wen and Peter C. Giardina should be considered as equal contributors in this work.

REFERENCES

1. Nassif, X., Pujol, C., Morand, P., and Eugene, E. (1999) *Mol. Microbiol. 32*, 1124−1132.
2. Harvey, H., Ketterer, M., Preston, A., Lubaroff, D. M., Williams, R., and Apicella, M. A. (1997) *Infect. Immun. 65*, 2420−2427.
3. McGee, Z., and Stephens, D. (1984) *Surv. Synth. Path. Res. 3*, 1−10.
4. McGee, Z., Stephens, D., Hoffman, L., d. Schlech, W., and Horn, R. (1983) *Rev. Infect. Dis. 5 (Suppl. 4)*, S708−S714.5.
5. Mosleh, I., Boxberger, H.-J., Sessler, M., and Meyer, T. (1997) *Infect. Immun. 65*, 3391−3398.
6. Nassif, X., and So, M. (1995) *Clin. Microbiol. Rev. 8*, 376−388.
7. Shaw, J., and Falkow, S. (1988) *Infect. Immun. 56*, 1625−1632.
8. Zenni, M. K., Giardina, P. C., Harvey, H. A., Shao, J., Ketterer, M. R., Lubaroff, D. M., Williams, R. D., and Apicella, M. A. (2000) *Infect. Immun.* (in press).
9. Giardina, P., Williams, R., Lubaroff, D. M., and Apicella, M. A. (1998) *Infect. Immun. 66*, 3416−3419.
10. Grassme, H., Ireland, R., and van Putten, J. P. M. (1996) *Infect. Immun. 64*, 1621−1630.
11. Merz, A. J., and So, M. (1997) *Infect. Immun. 65*, 4341−4349.
12. Pujol, C., Eugene, E., De Saint Martin, L., and Nassif, X. (1997) *Infect. Immun. 65*, 4836−4842.
13. van Putten, J. P. M., Duesing, T. D., and Carlson, J. (1998) *J. Exp. Med. 188*, 941−952.
14. Sandstrom, E. G., Napp, J. S., Reller, L. B., Thompson, S. E., Hook, E. W., and Holmes, K. K. (1984) *Sex. Trans. Dis. 11*, 77−80.
15. Bauer, J. F., Rudel, T., Stein, M., and Meyer, T. F. (1999) *Mol. Microbiol. 31*(3), 903−913.
16. Mosleh, M. I., Huber, L. A., Steinlein, P., Pasquali, C., Gunther, D., and Meyer, T. F. (1998) *J. Biol. Chem. 273*, 35332−35338.
17. Blake, M., and Gotschlich, E. (1987) in *Bacterial Outer Membranes as Model Systems* (Inouye, M., Ed.) pp 377−400, John Wiley & Sons, Inc., New York.
18. Lynch, E., Blake, M., Gotchlich, E., and Mauro, A. (1984) *Biophys. J. 45*, 104−107.
19. Weel, J., Hopman, C., and van Putten, J. P. M. (1991) *Pathogen. Gonoco. Infec. 174*, 705−715.
20. Weel, J., and van Putten, J. P. M. (1991) *Res. Microbiol. 142*, 985−993.
21. Biancone, L., Conaldi, P., Toniolo, A., and Camussi, G. (1997) *Exp. Nephrol. 5*, 330−336.
22. Bjerknes, R., Guttormsen, H., Solberg, C., and Wetzler, L. (1995) *Infect. Immun. 63*, 160−167.
23. Camussi, G., Biancone, L., Iorio, L., Silvestro, L., Da Col, R., Capasso, C., Rossano, F., Servillo, L., Balestrieri, C., and Tufano, M. (1992) *Kidney Int. 42*, 1309−1318.
24. Muller, A., Gunther, D., Dux, F., Naumann, M., Meyer, T. F., and Rudel, T. (1999) *EMBO J. 18*, 339−352
25. Tufano, M., Biancone, L., Rossano, F., Capasso, C., Baroni, A., De Martino, A., Ioria, E., Silvestro, L., and Camussi, G. (1993) *Eur. J. Immunol. 214*, 685−693.
26. Tufano, M., Ianniello, R., Galdiero, M., De Martino, L., and Galdiero, F. (1989) *Microb. Pathog. 7*, 337−346.
27. Tufano, M., Tetta, C., Biancone, L., Iorio, L., Baroni, A., Giovani, A., and Camussi, G. (1992) *J. Immunol. 149*, 1023−1030.
28. Carbonetti, N., and Sparling, P. (1987) *Proc. Natl. Acad. Sci. U.S.A. 84*(24), 9084−9088.
29. Gotschlich, E., Seiff, M., and Blake, M. (1987). *Proc. Natl. Acad. Sci. U.S.A. 84*, 8135−8139.
30. Smith, N., Smith, J., Maynard, and Spratt, B. (1995) *Mol. Biol. Evol. 12*, 363−370.
31. Cook, R. K., and Rubenstein, P. A. (1992) in *Practical Approachs in Cell Biology* (Carraway, K., and Carraway, C. C., Eds.) pp 99−122.
32. Strzelecka-Golaszewska, H., Moraczewska, J., Khaitlina, S. Y., and Mossakowska, M. (1993) *Eur. J. Biochem. 211*, 731−742.
33. Feng, L., Kim, E., Lee, W.-L., Miller, C. J., Kuang, B., Reisler, E., and Rubenstein, P. A. (1997) *J. Biol. Chem. 272*, 16829−16837.
34. Gotschlich, E. C., Blake, M. S., Lytton, E. J., and Seiff, M. (1987) *Antonie van Leeuwenhoek. 53*, 455−459.
35. Kouyama, T., and Mihashi, K. (1981) *Eur. J. Biochem.* 114, 33−38.
36. Cooper, J. A., Walker, S., and Pollard, T. D. (1983) *J. Musc. Res. Cell Motil. 4*, 253−262.
37. Mockrin, S. C., and Korn, E. D. (1981) *J. Biol. Chem.* 256, 8228−8233.
38. Knight, P., and Offer, G. (1978) *Biochem. J. 175*, 1023−1032.
39. Millonig, R., Salvo, H., and Aebi, U. (1988) *J. Cell Biol. 106*, 785−796.
40. Ng, R., and Abelson, J. (1980) *Proc. Natl. Acad. Sci. U.S.A. 77*, 2546−2550.
41. Kron, S. J., Drubin, D. G., Botstein, D., and Spudich, J. A. (1992) *Proc. Natl. Acad. Sci. U.S.A. 89*, 4466−4470.
42. Korman, V., Dixon, K., and Tobacman, L. (1999) *Biophys. J. 76*, A41
43. Holmes, K. C., Popp, D., Gebhard, W., and Kabsch, W. (1990) *Nature 347*, 44−49.
44. Lorenz, M., Popp, D., and Holmes, K. C. (1993) *J. Mol. Biol. 234*, 826−836.
45. Steinmetz, M. O., Stofler, D., Muller, S. A., Jahn, W., Wolpensinger, B., Goldie, K. N., Engel, A., Faulstich, H., and Aebi, U. (1998) *J. Mol. Biol. 276*, 1−6.
46. Combeau, C., and Carlier, M.-F. (1988) *J. Biol. Chem. 263*, 17429−17436.
47. Orlova, A., and Egelman, E. H. (1992) *J. Mol. Biol. 227*, 1043−1053.
48. Xu, X., Forbes, J. G., and Colombini, M. (1999) *Biophys. J. 76*, A143.
49. Shariff, A., and Luna, E. J. (1990) *J. Cell Biol. 110*, 681−692.
50. Chia, C. P., Hitt, A. L., and Luna, E. J. (1991) *Cell Motil. Cytoskel. 18*, 164−179.
51. Chia, C. P., Shariff, A., Savage, S. A., and Luna, E. J. (1993) *J. Cell Biol. 120*, 909−922.
52. Hitt, A. L., Hartwig, J. H., and Luna, E. J. (1994) *J. Cell Biol. 126*, 1433−1444.
53. Zhou, D., Mooseker, M. S., and Galan, J. E. (1999) *Science 283*, 2092−2095.
54. Zhou, D., Mooseker, M. S., and Galan, J. E. (1999) *Proc. Natl. Acad. Sci. U.S.A. 96*, 10176−10178.

BI000241J